


Article

# BioDT: An Integrated Digital-Twin-Based Framework for Intelligent Biomanufacturing

Beichen Zhao <sup>1,2</sup>, Xueliang Li <sup>1,2,3,\*</sup>, Wanqiang Sun <sup>1,2</sup>, Juntao Qian <sup>3</sup>, Jin Liu <sup>3</sup>, Minjie Gao <sup>4</sup>, Xin Guan <sup>1,2</sup> , Zhenwu Ma <sup>5</sup> and Jianghua Li <sup>2,4,\*</sup>

<sup>1</sup> Key Laboratory of Industrial Biotechnology, Ministry of Education, Jiangnan University, Wuxi 214122, China; zhaobeichen@stu.jiangnan.edu.cn (B.Z.)

<sup>2</sup> Science Center for Future Foods, Jiangnan University, Wuxi 214122, China

<sup>3</sup> T&J Bioengineering (Shanghai) Co., Ltd., Shanghai 201611, China

<sup>4</sup> Key Laboratory of Carbohydrate Chemistry and Biotechnology of Ministry of Education, School of Biotechnology, Jiangnan University, Wuxi 214122, China

<sup>5</sup> College of Mechanical Engineering, Suzhou University of Science and Technology, Suzhou 215009, China

\* Correspondence: bruce.li@jiangnan.edu.cn (X.L.); lijianhua@jiangnan.edu.cn (J.L.)

**Abstract:** The field of industrial biotechnology has shown an increasing interest in adopting digital twins for improving process productivity and management efficiency. Despite its potential benefits, digital-twin-based biomanufacturing has not been fully implemented. As a preliminary undertaking, we developed an open-source digital twin framework for cell culture. The core models of the digital twin were coded in C++ and compiled as a reusable Python library. A web-based, cloud-native HMI application that links the physical and virtual systems was developed. A microbioreactor digital twin system was implemented using the framework as a proof of concept. The system features a 3D-printed rocking platform that is customized to fit T25 flasks, enabling automated rocking rate and angle control and in-place optical cell density measurement. The digital twin was validated using Chinese Hamster Ovary (CHO) cells and was found to be able to predict the changes in cell density, glucose consumption, lactic acid production, and oxygen uptake rate (OUR). Finally, we performed a case study to demonstrate the system's practical applicability in Advanced Process Control (APC) by constructing real-time glucose and lactic acid soft sensors, which are in turn used to alert the operator for manual media change or for automated feeding.

**Keywords:** digital twin; advanced process control; process analytical technology; Chinese hamster ovary (CHO) cells; soft-sensor; 3D-printing; open-source software



**Citation:** Zhao, B.; Li, X.; Sun, W.; Qian, J.; Liu, J.; Gao, M.; Guan, X.; Ma, Z.; Li, J. BioDT: An Integrated Digital-Twin-Based Framework for Intelligent Biomanufacturing.

*Processes* **2023**, *11*, 1213. <https://doi.org/10.3390/pr11041213>

Academic Editor: Jochen Strube

Received: 15 March 2023

Revised: 5 April 2023

Accepted: 12 April 2023

Published: 14 April 2023



**Copyright:** © 2023 by the authors. Licensee MDPI, Basel, Switzerland. This article is an open access article distributed under the terms and conditions of the Creative Commons Attribution (CC BY) license (<https://creativecommons.org/licenses/by/4.0/>).

## 1. Introduction

The concept of Industry 4.0 has initiated a revolution in a number of industrial sectors. While digitalization emerges as a crucial step towards modernization in its own right [1], it also serves as the foundation to promote intellectualization. As of late, digitalization has gained significant attention and has had a profound impact on various process industries [2]. The rise of digital technologies has provided plenty of valuable tools to effectively manage voluminous data and make informed decisions in the production process. Given the progression of sensors [3], virtualization technology [4], and modelling [5], as well as the proliferation of computing power, simulation has emerged as a ubiquitous research methodology. By leveraging in silico modelling, comprehensive and precise digital replicas of entire manufacturing systems or product lifecycles can be constructed. With these technical prerequisites, the notion of digital twin (DT) attracted increasing interest from both academia and industry [6].

In 2003, Grieves introduced the notion of digital representation for tangible products in the context of product lifecycle management, which was an early exploration of what we now know as the digital twin [7]. In response to the growing demands of the aerospace

industry, NASA gave a comprehensive definition of digital twin in 2012. This definition presented an integrated multi-scale and multi-physics model, supported by physical models, feedback from sensors, and historical data, all of which work in concert to simulate the complete lifecycle of a physical system [8]. The Gartner Group's 2018 report recognized the digital twin as one of the top ten most promising technological trends of the time [9]. Subsequently, digital twins have been implemented in a wide range of applications, including but not limited to, manufacturing [10], medicine [11] and the process industry [12].

The concept of the digital twin introduced a novel paradigm of Cyber-Physical System (CPS), which operates on a foundation of multi-scale digital twins in conjunction with a physical manufacturing system. The fundamental constituents of a digital-twin-driven manufacturing system include a physical manufacturing system, corresponding digital twin, a Human–Machine Interface (HMI) application, and bidirectional data channels for seamless data exchange. A multitude of online sensors are embedded within the physical manufacturing system, allowing for the continuous monitoring and tracking of its status. The collected data are synchronized with the digital twin, which operate autonomously to simulate the current or future status of the manufacturing system. The HMI application is tasked with displaying sensor data and the digital twin's outputs in a coherent manner. Furthermore, the system operators possess the capability to alter manufacturing system parameters, subsequently triggering updates to both the digital twin and the predicted data that are in need of recalculation.

Despite the potential advantages of the digital twin, its implementation in the realm of biomanufacturing is facing a host of challenges. To achieve optimal levels of productivity, it is incumbent upon both the academic and industrial sectors to undertake the comprehensive digitization of biomanufacturing processes. Although the efficacy of digital twins has been demonstrated in myriad domains, their applications in biomanufacturing remains incipient owing to the complexities of biological systems [13] and the stringent safety requirements governing this field [14].

Udugama et al. [15] elaborated a three-tiered approach to constructing bioprocess digital twins, involving the digital model, the digital shadow, and ultimately, the digital twin. Whereas the digital model solely offers static prognoses of the bioprocesses, and the digital shadow merely reflects their actual status, the digital twin furnishes dynamic predictions based on mathematical models, executing self-iteration to enhance performance through the continued analysis of process data.

The domain of biomanufacturing has seen a proliferation of modelling methodologies, including computational fluid dynamics (CFD) [16], kinetics [17], and metabolic models [18], which have been extensively studied. Additionally, the feasibility of digital twins has been explored and validated through a series of studies focused on HIV-Gag VLP production in HEK293 cells [19–21], demonstrating their potential in optimizing processes and achieving autonomous process control. Furthermore, Park et al. [22] have discussed the essential technologies required to realize the bioprocess digital twin for Chinese hamster ovary (CHO) cell culture. However, despite these promising developments, there remains several critical areas that require further attention. For instance, there is a dearth of research concerning the updating of model parameters according to process data. Moreover, existing research is primarily focused on specific scenarios within narrow scopes, with a lack of emphasis on interoperability and reusability, hindering their adoption in biomanufacturing.

As an exploratory foray, we present BioDT, a digital-twin-based cell culture framework, which serves as an example of a digital-twin-based biomanufacturing system and offers a reference for future research. It is noteworthy that all components of this framework are open-source, enabling researchers to adapt it to diverse research scenarios. Furthermore, to elucidate the operational mechanisms of this framework, we designed a CHO cell culture microbioreactor based on it. Our design encompasses a 3D-printed automated microbioreactor, a bioprocess digital twin, and an HMI application. The microbioreactor is designed to support in-place cell density monitoring, and it is specifically adapted to accommodate T25 flasks, a widely used cell culture vessel. The bioprocess digital twin

was designed to take advantage of hybrid programming where C++ was used to encode the kinetic formulae of mass transfer, cell growth, and metabolism, while calculations and simulations were carried out in a Python program. The HMI application was also implemented in Python, and it is used to display process trends and provide users with an interface to interact with the system. The digital twin was validated by comparing the experimental data of cell density, glucose, and lactic acid concentrations with those predicted by the digital twin in CHO cell culture. To further illustrate the versatility of the system, we presented a case study of manual media change and automated glucose feeding. Results indicate that the digital twin provided reliable reference values of metabolite concentrations, and showed its potential in Advanced Process Control (APC).

## 2. Materials and Methods

### 2.1. Cell Culture and Sampling

Our laboratory preserved the cell line of FreeStyle™ CHO (Thermo Fisher Scientific, Waltham, MA, USA) for suspension culture. The culture was conducted in a T25 flask (Thermo Fisher Scientific, Waltham, USA) at 37 °C and 8% CO<sub>2</sub> within an incubator using FreeStyle™ CHO Expression Media (Thermo Fisher Scientific, Waltham, USA), supplemented with 8 mM glutamine. The culture volume was 10 mL. Given the weaker shear stress present in rocking T25 flasks compared to other culture vessels [23], 0.2% of the Anti-Clumping Agent (Thermo Fisher Scientific, Waltham, USA) was incorporated into the media to prevent cell clumping. The T25 flask was secured onto a 3D-printed platform driven by a stepper motor at a predetermined speed and angle. The in-place measurement of cell density was executed every 15 min using a pair of near-infrared emitter and receiver, while glucose and lactic acid concentration levels were sampled every 12 h with a biological analyzer (Sieman Technology, Shenzhen, China).

### 2.2. 3D-Printed Automated Microbioreactor with Real-Time Cell Density Measurement

Many automated miniature-scale devices have been developed for cell or bacterial cultures. One notable example is eVOLVER, presented by Wong et al. [24], which enables fine-tuning of a few process parameters and supports high-throughput operation. However, despite these advancements, most cell culture devices merely record process parameters and fail to meet the crucial requirement of real-time communication with models, which is a fundamental characteristic of the digital twin. In this study, we designed and 3D-printed an automated microbioreactor for the cultivation of CHO cells in T25 flasks (Figure 1a–c). Our design incorporates the capability of adjusting the rocking speed and angle, as well as monitoring the cell density in place. Importantly, the device is also equipped with a Wi-Fi chip that enables data exchange with a digital twin, thus facilitating the continuous updating of process parameters and monitoring of system status, supporting the implementation of the digital twin in terms of hardware.

The 3D model of the device was designed using Autodesk Fusion 360 and realized by a 3D printer (Creative 3D) with PLA filament. All electronic components were connected to an Arduino UNO board (Smart Projects, Pescara, Italy) as the micro controller. The controller board consisted of five modules: (1) a Wi-Fi chip for communication with the HMI, enabling data transmission and receipt of commands. (2) A stepping motor for rocking the T25 flask, which was powered and controlled by an encoder board wired to the Arduino. The motor allowed for adjustable rocking speeds from 40 to 80 rpm and angles of 0–90° (typical range is 7–15°). (3) An acceleration sensor for monitoring the rotation speed and angle of the flask by detecting the vertical component of gravity. However, the rocking action was not based on the real-time output from the acceleration sensor in a feedback loop manner. Instead, the acceleration sensor was only used to adjust the initial position of the flask before rocking commenced. Afterwards, the rocking angle and velocity were open-loop-controlled by taking advantage of the stepper motor's precise discrete motion. During cell density measurements, the motor firstly levels the flask, then rotates it by 90° (Figure 2a), collecting the liquid at the bottom of the flask. After the optical measurement,

the flask is rotated back to its initial position and the rocking resumes. (4) A coupled 940 nm near-infrared emitter and receiver (Figure 2b) were utilized to measure the intensity of light passing through the media, thereby assessing the optical density of the culture. (5) A 16-bit analog–digital (AD) converter was used to convert the analog signal to amplified digital signal (Figure 2d), which can be interpreted by Arduino. The optical density was converted to cell density using a predefined calibration curve (Figure 2c). Since signals can fluctuate during sampling, which can lead to noise and inaccuracies in the data, a Kalman filter was utilized to reduce the noise. The Kalman filter is designed to analyze the current and past values of a signal and calculate the optimal estimate of the signal's true value.

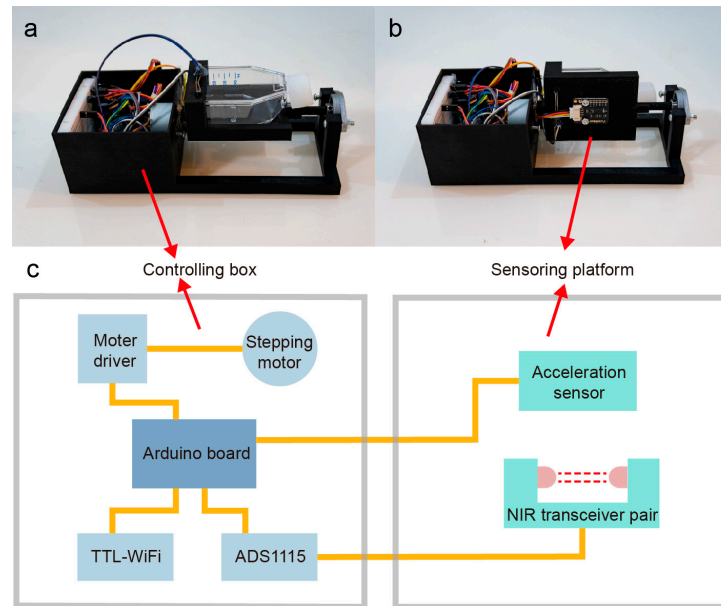


**Figure 1.** Design of a rocking microbioreactor. (a) Front view with the T25 flask in place. (b) Bottom view of the sensing platform, showing the acceleration sensor. (c) Connection diagram of electronic components.

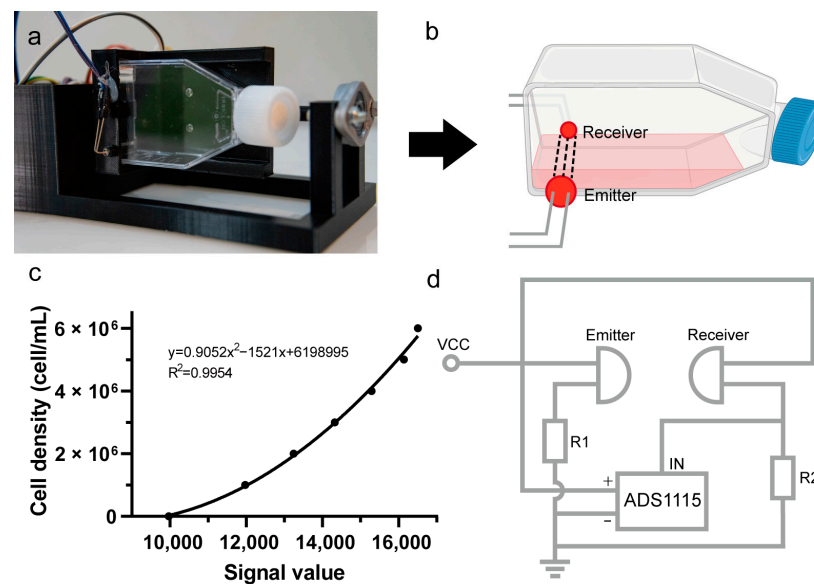


**Figure 2.** The working principle of the optical sensor. (a) The platform's posture when cell density detection was performed. (b) Location of the emitter and receiver on the microbioreactor. (c) Calibration curve of cell density and signal values. (d) Circuit schematic of the optical sensor and the AD converter.

### 2.3. Bioprocess Simulation

For the modelling part, we introduce Pyrex, a Python library for bioreaction computing currently remaining in development, which we anticipate to be a valuable resource for researchers. To provide a preview of its capabilities, we present a simplified version of it in the context of CHO cell culture. To accurately track the CHO cell growth and metabolism, we incorporated a set of commonly used kinetics equations with parameters obtained through batch culture experiments and the literature.

The cell growth rate is calculated using a logistic equation (Equation (1)). The initial value of  $\mu_{max}$  of  $0.05 \text{ h}^{-1}$  is acquired from the literature [25], and it is updated along with the sensor data. The maximum cell density,  $X_{max}$  is set to  $8 \times 10^6$  according to batch culture experiments. It should be noted that the use of the logistic equation is for demonstration purposes only. Other types of empirical or mechanistic equations can be readily incorporated.

$$\mu = \mu_{max} \cdot \left(1 - \frac{X}{X_{max}}\right) \quad (1)$$

where  $\mu$  is the specific growth rate (cell/cell);  $\mu_{max}$  is the maximum growth rate (cell/cell);  $X$  is the cell density (cell/mL);  $X_{max}$  is the maximum cell density (cell/mL).

The consumption rate of glucose and the generation of lactic acid are carried out using Equations (2) and (3). The initial values of  $q_{glu}$  and  $Y_{lac/glu}$  were estimated from batch experiments, which were  $-2.06 \times 10^{-13} \text{ L/g/cell/h}$  and  $0.46$ , respectively.

$$\frac{dS_{glu}}{dt} = q_{glu} \cdot S_{glu} \cdot X \quad (2)$$

$$\frac{dS_{lac}}{dt} = Y_{lac/glu} \cdot \frac{dS_{glu}}{dt} \quad (3)$$

where  $S_{glu}$  is the concentration of glucose (g/L);  $S_{lac}$  is the concentration of lactic acid (g/L);  $q_{glu}$  is the specific glucose consumption rate (L/g/cell/h);  $Y_{lac/glu}$  is the yield coefficient of lactate to glucose (g/g).

As these two parameters continuously evolve with the environmental conditions and the physiological status of the cells, they were re-evaluated by the digital twin using the process data, as described later.

To consider the variations in dissolved oxygen during cell culture, the oxygen transfer rate and the oxygen uptake rate were calculated, respectively. The relationship between the rocking speed and the volumetric mass transfer coefficient,  $k_L a$ , was previously determined by Liu et al. [23] at an interval of 10 rpm and an amplitude of  $7^\circ$ . We use a polynomial function, Equation (4), to fit these data to estimate the  $k_L a$  at any rocking speed between 10 and 80 rpm. The oxygen saturation concentration was set to  $0.25 \text{ mol/L}$ , i.e., 92% of that in equilibrium with air at atmosphere pressure, as the incubator has 8% of  $\text{CO}_2$  in it. The value of  $q_{O_2}$  was set to  $3.2 \times 10^{-13} \text{ mol/cell/h}$  according to Deshpande et al. [26]. The value of dissolved oxygen was then calculated with Equation (5).

$$k_L a = 0.0016\omega^2 + 0.124\omega + 2.6279 \quad (4)$$

$$\frac{dC_L}{dt} = (k_L a(C^* - C_L) - q_{O_2} \cdot X) \cdot dt \quad (5)$$

where  $k_L a$  is the volumetric mass transfer coefficient ( $\text{h}^{-1}$ );  $\omega$  is the rocking speed;  $C_L$  is the dissolved oxygen concentration (mmol/L);  $C^*$  is the equilibrium oxygen concentration (mmol/L); and  $q_{O_2}$  is the specific glucose consumption rate (mmol/cell/h).

Given that analytical solutions for different differential equations are not universally achievable, numerical methods were employed to integrate these equations with a step-size of 1 s. As the cell metabolism is relatively slow, process parameters are not expected to experience significant changes over such a short period of time; the system's status can

thus be assumed to be in quasi-steady state at each time step. This approach ensures that the system's state is updated every second. It should be noted that if a larger time interval is used or for a fast-changing system, a higher-order scheme should be adopted to reduce numerical errors.

In order to optimize computing performance, all of the above-mentioned formulae were coded in C++. The C++ code was then compiled as a Python extension using Pybind11, thereby allowing for the execution of these C++ functions by Python applications for flexibility. A Python program was subsequently created to integrate these methods, enabling real-time data processing, realizing the implementation of the digital twin. Parameters were updated once sensor data or offline measurement were synchronized to the digital twin. The Levenberg–Marquardt algorithm included in the Python package Scipy was used to recalculate the kinetic parameters.

#### *2.4. HMI Application*

To effectively manage data, seamlessly integrate predictive and decision-making functionalities, and facilitate user interactions, a simple Human–Machine Interface (HMI) was created in Python. The application comprises four modules: data transmission, data storage (SQL database), the digital twin, and data visualization. The data transmission module communicated with the device based on the TCP/IP protocol. The module created a socket and connected to the device through a soft serial port created by the Arduino at the IP address 192.168.4.1 and the port number 9000 as required by the Wi-Fi chip. The data transmission happened on-demand whenever the status of the device or the digital twin changed. The data storage module is based on SQLite, recording the sensor data and the digital twin's predictions. The digital twin module is based on the previously mentioned python extension named Pyrex. This module updates the predicted status in real time and iteratively corrects the model parameters when the device receives sensor data. Data visualization and user interface (UI) are based on the Python package bokeh (V2.3). The UI shows the data recorded by the device and predicted by the digital twin. Commands are sent to the digital twin or physical twin when the operator interacts with the HMI. Detailed usage of the HMI can be found in our published codes on GitHub.

#### *2.5. Integration of the Digital-Twin-Based Cell Culture Framework*

Through the integration of the aforementioned components, a digital-twin-based cell culture system was realized, as depicted in Figure 3. This innovative framework seamlessly linked the hardware and software, as well as the virtual replica and physical device, in accordance with the BioDT paradigm. The bidirectional data flow between the system components facilitated the optimal utilization of data, thereby enhancing the accuracy and efficiency of the system.

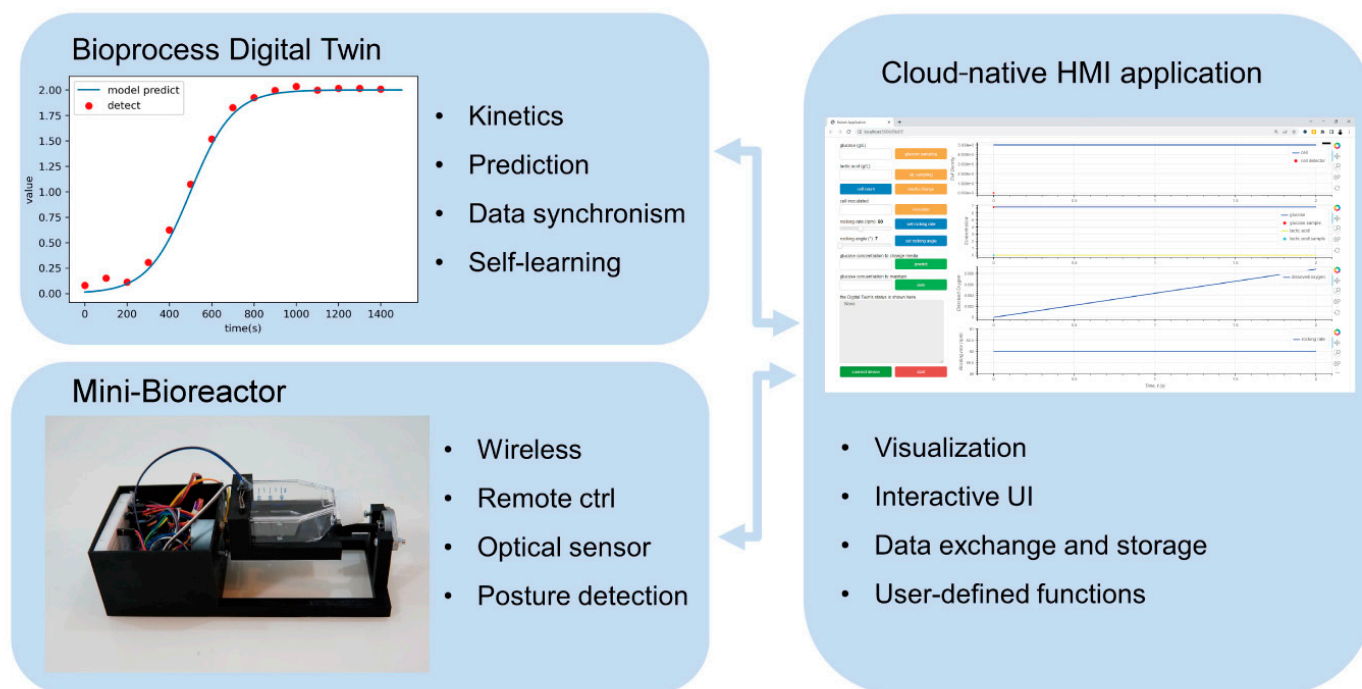


**Figure 3.** The architecture of the digital-twin-based cell culture system.

### 3. Results

#### 3.1. Validation of the Microbioreactor and Sensors

Cell growth was monitored via an optical sensor that takes measurements every 15 min. However, due to mechanical vibrations and the ubiquitous existence of electromagnetic interference in the laboratory environment, noise existed in the sensor's readings. To address this issue, we applied the Kalman filter, which was proven to be able to significantly reduce the noise. As illustrated in Figure 4a, the denoised data showed excellent agreement with offline measurement sampled during the experiments. Based on these results, the data collected via the optical sensor were validated and deemed suitable for use in the subsequent research.

To validate the feasibility of cell cultivation in this device, experiments under different rocking speeds and angles were carried out and the variations in cell density were recorded. The microscope images show that the cells cultured in this device are in good morphological status (Figure 4e). Figure 4c,d demonstrate that the rate of cell growth is positively correlated with the rocking speed. However, the changes of rocking angle did not bring such differences. In an attempt to interpret these findings, the dissolved oxygen was calculated throughout the cultivation using Equation (5) with reported parameters at an angle of  $7^\circ$ , using an initial cell density of  $5 \times 10^6$  cell/mL. The simulation results, as shown in Figure 4b, indicate that the dissolved oxygen saturation remained above 99%, with differences only in the initial rate of reaching this level. However, it is notable that the hindrance to oxygen mass transfer by filter membranes could be more crucial in T25 flasks [23] and may become a potential factor that influences the cell growth. Due to the lack of a dissolved oxygen (DO) sensor, which is able to measure the amount of oxygen that is dissolved in the media, we did not examine in detail the relationship between the dissolved oxygen and cell growth rate.

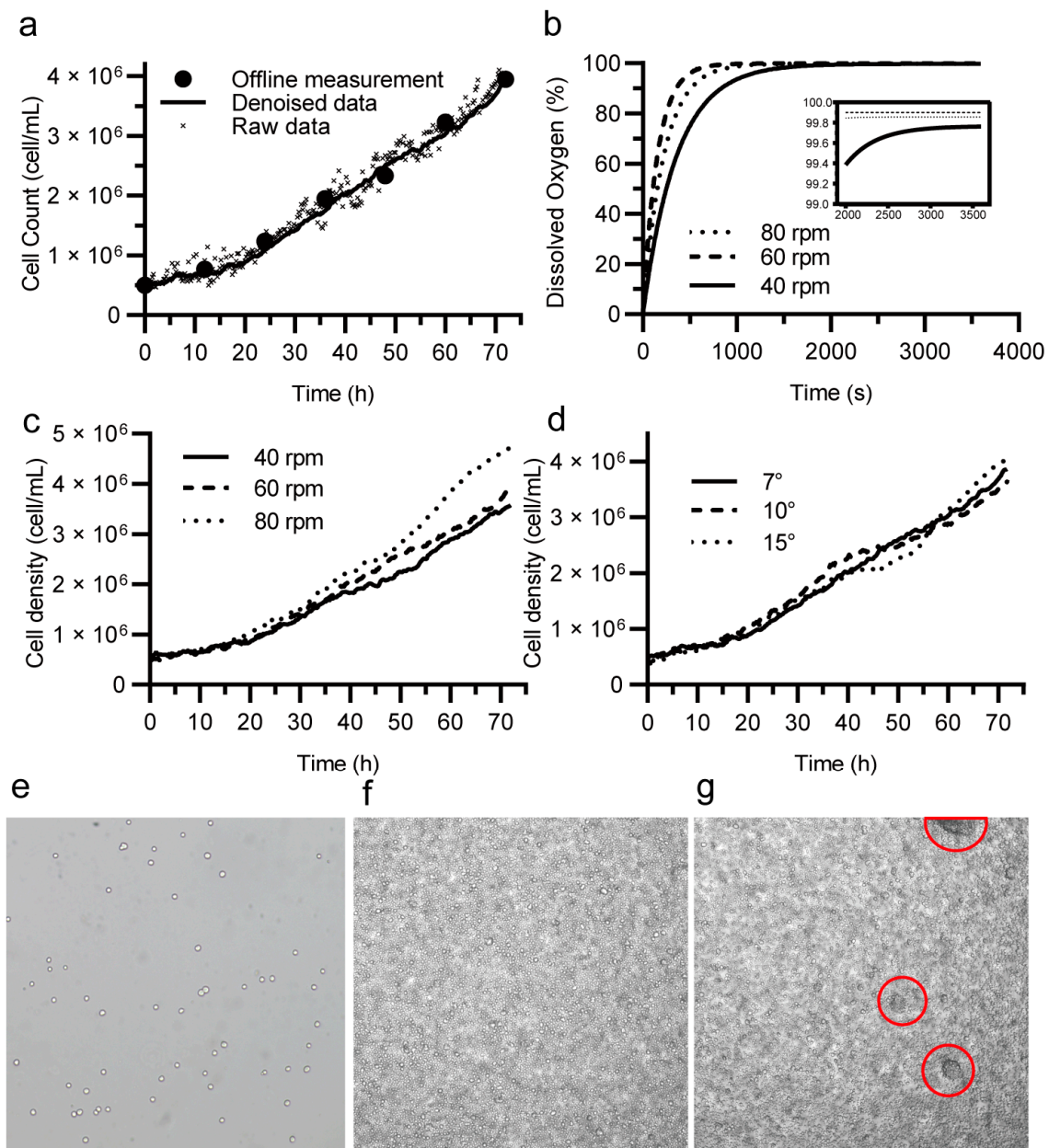


**Figure 4.** (a) Validation of the cell density sensor with a Kalman filter. (b) Simulation results of changes in dissolved oxygen at 40, 60 and 80 rpm and 7° rocking angle. (c) Changes in cell density at 40, 60 and 80 rpm and 7° rocking angle. (d) Cell growth at 7°, 10° and 15° rocking angle and 60 rpm speed. (e) Microscopic image of cells' morphological status. (f) Microscopic image of cells performing periodical 90° rotation. (g) Microscopic image of cells not performing periodical 90° rotation.

We also found that the 90° rotation of the flask during the cell density detection had beneficial effects in preventing cell clumping. The turbulence in the rocking flask is comparatively less intensive than other conventional culture techniques, such as the TPP tube which requires a spinning speed of 180 rpm, and the shake flask which necessitates a spinning speed of 120 rpm. Although the anti-clumping agent was added to the media, clumps of cells were still observed when we cultured the cells without rotating as Figure 4f,g show. This mechanism may alleviate the clustering for other cell lines with high adhesion property.



### 3.2. Validation of the Digital Twin

In order to evaluate the performance of the digital twin, a 72 h cell culture experiment was conducted, considering the potential effects of fluctuations in environmental conditions and substrate concentrations on cell growth. Media change was carried out at the 36 h mark, in order to simulate the impact of such changes on cell growth.

To clearly illustrate the advantages of the digital twin over the digital model and the digital shadow, we compared the predictions of cell growth, glucose consumption and lactic production using these three methods. As previously mentioned, a digital model statically predicts the culture status of the whole process according to the given initial condition and model parameters. The digital shadow updates the status according to the sensor or sampling data. This allows the digital shadow to be better synchronized with the status. However, as cell culture is highly susceptible to a variety of factors, the digital shadow cannot track the variation of kinetics, which eventually results in accumulated error. Once synchronized with sensor and sampling data, the digital twin iteratively updates the parameters included in the kinetics equations. Thus, if the kinetic properties of cell growth and metabolism are altered, they can be readily captured by the digital twin.

The evolution of the cell density during a run was estimated by the digital model, the digital shadow and the digital twin, respectively. As can be seen in Figure 5a, the static predictions from the digital model deviated from the experimental data slightly at the beginning, but the error increased as time passed. This discrepancy can be attributed to the inability of the kinetic equations' parameters to precisely describe the specific conditions of the entire run, leading to accumulated errors that cannot be eliminated. The digital shadow and the digital twin were synchronized with the sensor data and corrected errors every 15 min, resulting in a more accurate estimation. In addition, the changes in specific growth rate (Figure 5d) were also provided by the digital twin as this value was updated once the sensor data were transmitted back. For the sole purpose of tracking process parameters, the advantage of the digital twin over the digital shadow is not apparent at high sampling frequencies. If the sensor were intentionally blocked and only the offline measurements of cell density were available, the digital twin would provide more precise predictions as it is able to trace the changes in kinetics (Figure 5g).

The glucose consumption and lactic acid production were also predicted by the digital model, the digital shadow and the digital twin, as Figure 5b,c show. The digital twin, which was recalibrated based on the acquired data, successfully captured the variation in the concentrations of glucose and lactic acid, leading to more accurate predictions compared to those obtained using the digital model and the digital shadow. The rates of glucose consumption and lactic acid generation were also calculated by taking advantage of the digital twin, showing an overall decreasing trend over time (Figure 5e,f). This phenomenon may be attributed to a reduction in metabolic activity due to a decrease in glucose concentration and an increase in cell density. These calculations showed the capabilities of the digital twin in tracing the metabolism of cells, which is particularly useful in understanding cell activities in dynamic situations.

Figure 5h,i present the process trends of the glucose and lactic acid concentrations, which were recalculated using the updated parameters obtained through the utilization of the digital twin. This approach is of great significance since the offline data only reflect the progress of the culture at discrete points in time. By reconstructing the entire culture process, the digital twin enables researchers to investigate the historical process more comprehensively, providing a more detailed and accurate understanding of the biological system being studied.

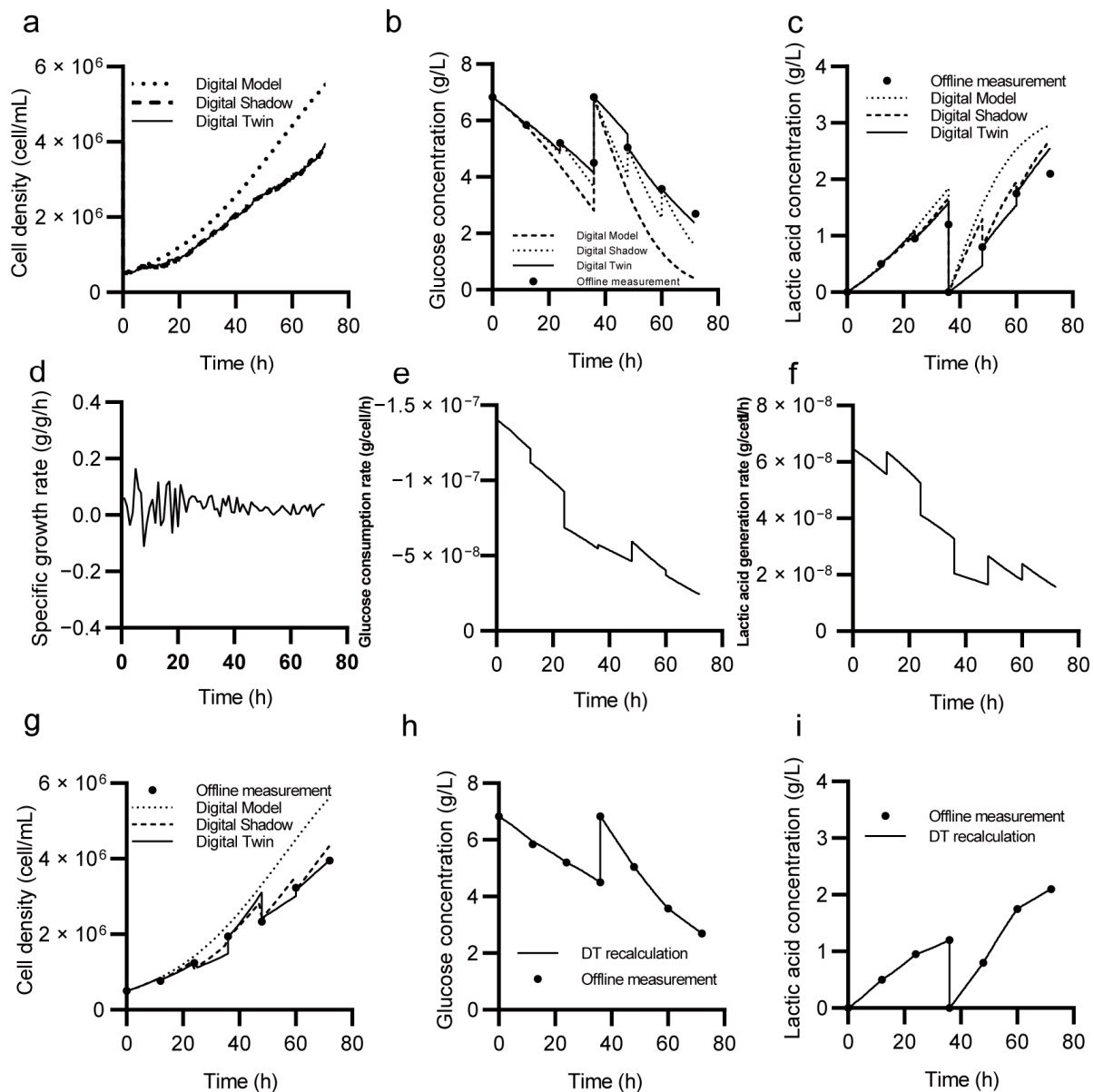


**Figure 5.** (a–c,g) Comparison between the predictions of the digital model, the digital shadow and the digital twin on cell density, glucose and lactic acid concentration. (d–f) Changes tracked by the digital twin on the specific growth rate, glucose consumption rate and lactic acid generation rate over time. (h,i) Comparison between recalculated data and sampling data of glucose and lactic acid concentrations.

### 3.3. Case Study

Biomanufacturing is a complex process that requires sophisticated process control in order to achieve consistent and high-quality products. The digital twin is a promising tool for achieving this goal, as it provides a virtual model of the manufacturing process that can be used for Advanced Process Control (APC). Here, we present a case study that demonstrates the advantages of using digital twins in the context of media supplement in cell cultivation processes.

To begin with, we integrated a function into the HMI that reminds the operators to change the media when the concentration of glucose or lactic acid reaches a preset value, for instance, 4 g/L glucose and 1 g/L lactic acid. We conducted several culture experiments with different initial inoculation densities of 20, 50, and 100 ( $\times 10^5$  cell/mL). The media was changed when the predicted concentration reached the preset values, and sampling was

carried out to validate the accuracy of the digital twin's predictions and to provide data for the digital twin's parameter iterations. As shown in Figure 6, the digital twin was able to provide a reliable reference for the concentrations and accurately predict the variation with different initial inoculation densities. Compared to the feeding strategies that are based on experience or at fixed intervals, the digital-twin-based system showed its potential in rational decision-making.

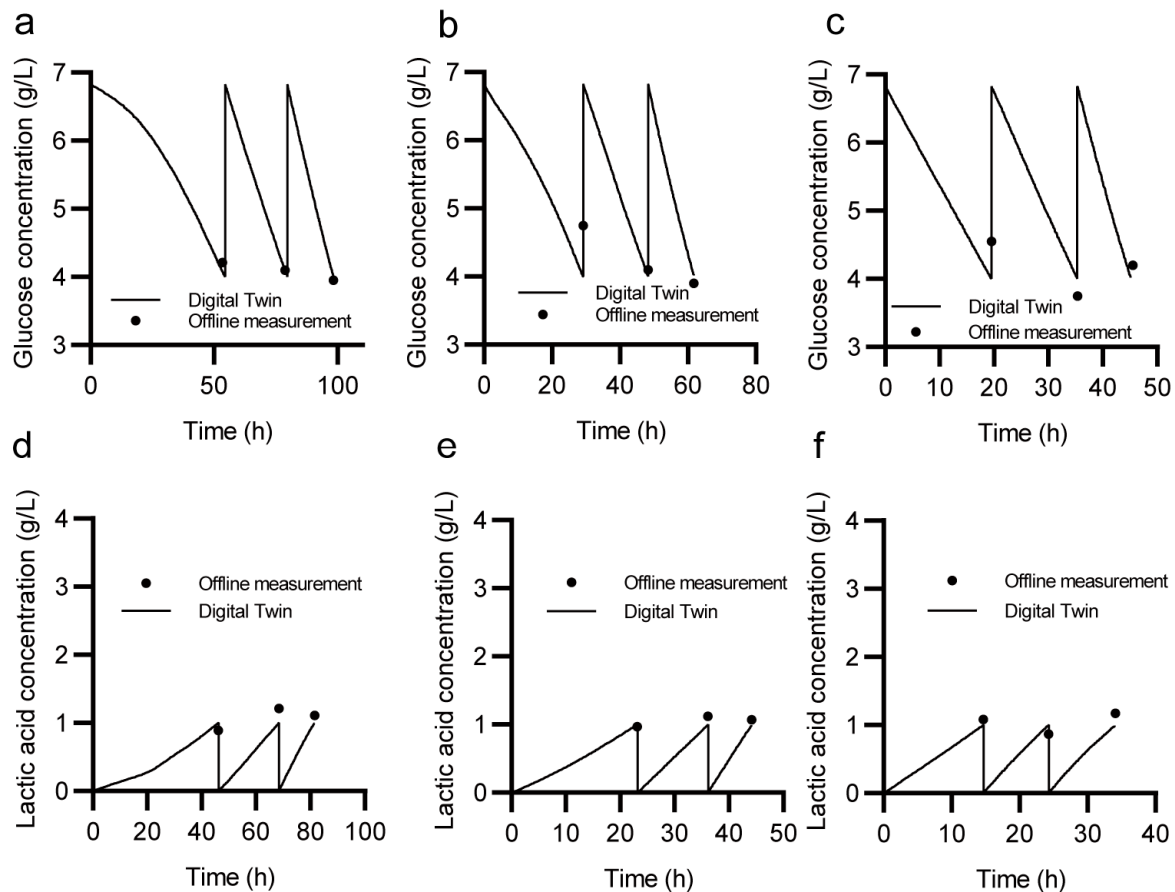


**Figure 6.** (a–c) Prescriptions of media change based on glucose concentration prediction at initial cell densities of 20, 50, and 100 ( $\times 10^5$  cell/mL). (d–f) Prescriptions of media change based on lactic acid concentration predictions with initial cell densities of 20, 50, and 100 ( $\times 10^5$  cell/mL).

In addition to the manual media change, we also implemented an automated glucose feeding system using a dosing pump as shown in Figure 7a. A miniature peristaltic pump was controlled by an electromagnetic relay, which received orders from the Arduino. A stock glucose solution at 50 g/L was drawn by the pump periodically, based on the predicted glucose concentration. Each pulse of the pump lasted 30 milliseconds, delivering 1 drop of concentrated glucose of about 0.05 mL. The inlet of the bottle was connected to the atmosphere via a 0.22-micron filter to balance the air pressure. As the changes in liquid volume due to feeding was small, the model was not updated to consider the volume change in the current study.

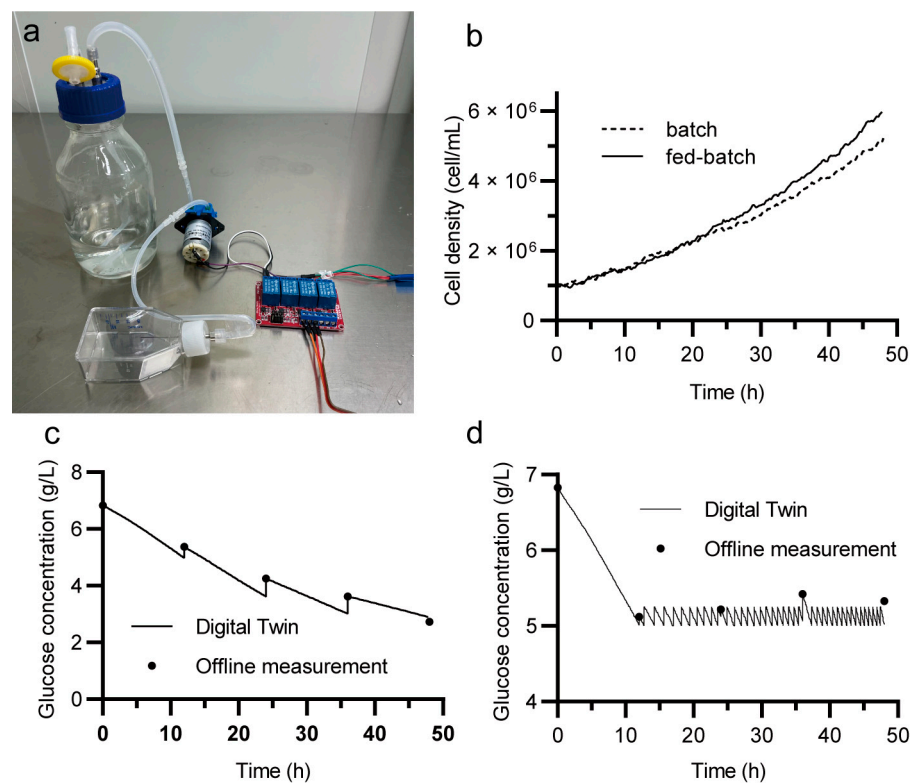


**Figure 7.** (a) Components and connections of the automated feeding system. (b) Cell densities in the batch and batch-fed cultures. (c) Evolution of the glucose concentration in the batch culture. (d) Changes of glucose concentration in the automated fed-batch culture.

Preliminary results in Figure 7c,d show that as the cell density increases, glucose feed becomes more frequent as a result of faster consumption rate. While the glucose concentration in the batch culture continued to decrease, the fed-batch culture was able to maintain the glucose concentration at the predetermined level over an extended period of time, eventually leading to an improvement in cell density of 14.8% (Figure 7b). It should be noted that this experiment was meant to be illustrative rather than comprehensive. The feeding strategy was not optimized, and the glucose concentration might not have been a limiting nutrient in the process. Nonetheless, precise control of the feeding rate and nutrient concentrations provides researchers with greater flexibility in optimizing cell growth conditions.

#### 4. Discussion

The present study details the development of a customizable and comprehensive digital-twin-based framework for cell culture, referred to as BioDT. This framework represents a standard paradigm for digital-twin-based cell culture and can serve as a reference for subsequent investigations in the field. To demonstrate the efficacy of the framework, we established a laboratory-scale CHO cell culture system using BioDT.

The design presented in this study consists of three key components: an innovative cell culture device, a digital twin, and a web HMI. The cell culture device is a miniature bioreactor that accommodates a T25 flask, featuring in-place monitoring of cell density and adjustable rocking speed and angle. A digital twin was constructed on a set of kinetic equations, which are used to calculate cell growth rate, glucose consumption, lactic acid production, and oxygen transfer. The HMI managed the exchange of data between the physical device and the digital twin, delivering real-time visualization of data, user interaction, and storage of data in a database. Through communication between the device and software, this system enabled dynamic and precise control over process parameters. The effectiveness of the proposed design was validated through a series of

cell culture experiments. With the assistance of the digital twin in kinetics tracing and process predicting, a more comprehensive and deeper understanding of bioprocesses can be achieved, which would be considerably useful in optimizing the production process.

The current system consists of highly customizable components, and we have made all blueprints and codes open-source, thereby exemplifying a flexible approach for digital-twin-based systems. The hardware component of our design is tailored for suspension culture in a T25 flask. However, any culture device that is adapted to the communication protocol can be integrated into the system, and the model equations can be readily modified to suit other type of reactors. A major drawback of the current physical system is the lack of sensors, unlike commercial manufacturing facilities that are equipped with more advanced process analytics. It should be reasonable to expect that the digital twin can be significantly enhanced in the latter case, which would in turn accelerate the digitization of biomanufacturing. We also designed the bioprocess modelling library Pyrex in C++, which ensures high computing performance, and can be utilized by any Python application. The library currently provides modelling methods for cell behavior and mass transfer, albeit in a limited capacity. To handle the complicated phenomena in biomanufacturing, from upstream to downstream, methods that consider more parameters and their interactions need to be developed. Hartmann et al. [27] comprehensively reviewed the modelling methods in bioprocesses and emphasized the necessity to develop multi-scale and multi-disciplinary models. Wang et al. [28] proposed that models that integrate spatiotemporal multiscale cellular models and fluid dynamics would be an ideal tool for bioprocess design as well. It is also of critical importance to create a widely applicable computing library for bioprocess modelling that can help drive digitization in biomanufacturing, which would be the focus of our subsequent research. By making appropriate modifications to the HMI, users can develop new features to adapt to their own culture system. Incorporating more sophisticated concepts and technologies related to Process Analytical Technology (PAT) and Advanced Process Control (APC) into this system would hold great promise for the widespread implementation of digital twins in biomanufacturing. This could eventually lead to improvements in productivity and quality control, bolstering the overall efficiency of the biomanufacturing process.

## 5. Conclusions

In this study, we presented a digital twin framework for intelligent biomanufacturing, called BioDT. A cell culture system was developed based on it, which incorporated a micro-bioreactor (physical twin), a digital twin and an HMI application. The proposed design was found to be effective in predicting variations in cell density, glucose consumption, and lactic acid production, along with the capability to trace the changes in kinetic parameters. As a case study to demonstrate the practical applicability of the digital twin, we realized a function to remind the operator to replenish the media after a metabolite concentration reached a preset value. With the addition of a dosing pump, this system enabled automated glucose feeding, resulting in a 14.8% improvement in cell density, compared to a batch culture. These findings highlighted the potential of the digital twin in Advanced Process Control (APC). The framework was made open-source to promote the development of the digital twin in biomanufacturing.

**Author Contributions:** Conceptualization, B.Z., X.L., J.L. (Jianghua Li) and M.G.; methodology, B.Z., X.L. and W.S.; software, B.Z., X.L. and Z.M.; validation, B.Z., X.L. and W.S.; formal analysis, B.Z. and X.L.; investigation, B.Z., X.L. and W.S.; resources, J.L. (Jianghua Li), X.G., Z.M., M.G., J.Q. and J.L. (Jin Liu); data curation, B.Z. and X.L.; writing—original draft preparation, B.Z.; writing—review and editing, X.L., J.L. (Jianghua Li), M.G. and X.G.; visualization, B.Z. and X.L.; supervision, J.L. (Jianghua Li), X.L., X.G., M.G., J.Q. and J.L. (Jin Liu); project administration, J.L. (Jianghua Li), X.L., M.G. and X.G.; funding acquisition, J.L. (Jianghua Li), X.L., X.G. and M.G. All authors have read and agreed to the published version of the manuscript.

**Funding:** This work was funded by the National Key R&D Program of China (2021YFC2101100), the Starry Night Science Fund of Zhejiang University Shanghai Institute for Advanced Study (SNZJU-SIAS-0013), and the Innovative Research Groups Project of the National Natural Science Foundation of China (32021005).

**Institutional Review Board Statement:** Not applicable.

**Informed Consent Statement:** Not applicable.

**Data Availability Statement:** The data presented in this study are available upon request from the corresponding author. All the codes used in this work are publicly available at <https://github.com/BeichenZhao/BioDT> (accessed on 14 March 2023).

**Conflicts of Interest:** T&J Bioengineering (Shanghai, China) has an interest in commercializing the technology described in this work. The authors declare no conflict of interest.

## Nomenclatures

$k_L a$	Volumetric mass transfer coefficient ( $\text{h}^{-1}$ )
$\mu$	Specific growth rate (cell/cell)
$\mu_{max}$	Maximum growth rate (cell/cell)
$X_{max}$	Maximum cell density (cell/mL)
$X$	Cell density (cell/mL)
$S_{glu}$	Concentration of glucose (g/L)
$S_{lac}$	Concentration of lactic acid (g/L)
$q_{glu}$	Specific glucose consumption rate (L/g/cell/h)
$Y_{lac/gluc}$	Yield coefficient of lactate to glucose (g/g)
$q_{O_2}$	Specific oxygen consumption rate (mmol/cell/h)
$C^*$	Equilibrium oxygen concentration (mmol/L)
$C_L$	Dissolved oxygen concentration (mmol/L)
$\omega$	Rocking speed

## References

- Lu, Y. Industry 4.0: A survey on technologies, applications and open research issues. *J. Ind. Inf. Integr.* **2017**, *6*, 1–10. [CrossRef]
- Tao, F.; Zhan, H.; Liu, A.; Nee, A.Y.C. Digital Twin in Industry: State-of-the-Art. *IEEE Trans. Ind. Inform.* **2019**, *15*, 2405–2415. [CrossRef]
- Gruber, P.; Marques, M.P.C.; Szita, N.; Mayr, T. Integration and application of optical chemical sensors in microbioreactors. *Lab A Chip* **2017**, *17*, 2693–2712. [CrossRef]
- Posada, J.; Toro, C.; Barandiaran, I.; Oyarzun, D.; Stricker, D.; De Amicis, R.; Pinto, E.B.; Eisert, P.; Dollner, J.; Vallarino, I. Visual Computing as a Key Enabling Technology for Industrie 4.0 and Industrial Internet. *IEEE Comput. Graph. Appl.* **2015**, *35*, 26–40. [CrossRef]
- Smiatek, J.; Jung, A.; Bluhmki, E. Towards a Digital Bioprocess Replica: Computational Approaches in Biopharmaceutical Development and Manufacturing. *Trends Biotechnol.* **2020**, *38*, 1141–1153. [CrossRef]
- Qi, Q.; Tao, F.; Hu, T.; Anwer, N.; Liu, A.; Wei, Y.; Wang, L.; Nee, A.Y.C. Enabling technologies and tools for digital twin. *J. Manuf. Syst.* **2021**, *58*, 3–21. [CrossRef]
- Grieves, M. Digital twin: Manufacturing excellence through virtual factory replication. *White Pap.* **2014**, *1*, 1–7.
- Glaessgen, E.; Stargel, D. The digital twin paradigm for future NASA and US Air Force vehicles. In Proceedings of the 53rd Structures, Structural Dynamics, and Materials Conference, Honolulu, HI, USA, 23–26 April 2012; p. 1818.
- Augustine, P. The industry use cases for the Digital Twin idea. *Digit. Twin Paradig. Smarter Syst. Environ. Ind. Use Cases* **2020**, *117*, 79–105. [CrossRef]
- Zambal, S.; Eitzinger, C.; Clarke, M.; Klintworth, J.; Mechin, P.-Y. A digital twin for composite parts manufacturing: Effects of defects analysis based on manufacturing data. In Proceedings of the 2018 IEEE 16th International Conference on Industrial Informatics (INDIN), Porto, Portugal, 18–20 July 2018; pp. 803–808.
- Martinez-Velazquez, R.; Gamez, R.; El Saddik, A. Cardio Twin: A Digital Twin of the human heart running on the edge. In Proceedings of the 2019 IEEE International Symposium on Medical Measurements and Applications (MeMeA), Istanbul, Turkey, 26–28 June 2019; pp. 1–6.
- Al-Sharrah, G.; Elkamel, A.; Almansoor, A. Sustainability indicators for decision-making and optimisation in the process industry: The case of the petrochemical industry. *Chem. Eng. Sci.* **2010**, *65*, 1452–1461. [CrossRef]
- Gargalo, C.L.; de Las Heras, S.C.; Jones, M.N.; Udugama, I.; Mansouri, S.S.; Krühne, U.; Gernaey, K.V. Towards the development of digital twins for the bio-manufacturing industry. *Digit. Twins Tools Concepts Smart Biomanuf.* **2021**, *176*, 1–34. [CrossRef]
- Braun, M. Represent me: Please! towards an ethics of digital twins in medicine. *J. Med. Ethics* **2021**, *47*, 394–400. [CrossRef] [PubMed]

15. Udugama, I.A.; Lopez, P.C.; Gargalo, C.L.; Li, X.; Bayer, C.; Gernaey, K.V. Digital Twin in biomanufacturing: Challenges and opportunities towards its implementation. *Syst. Appl. Microbiol.* **2021**, *1*, 257–274. [[CrossRef](#)]
16. Zhang, J.; Li, X.; Liu, H.; Zhou, J.; Chen, J.; Du, G. Hydrodynamics and mass transfer in spinner flasks: Implications for large scale cultured meat production. *Biochem. Eng. J.* **2021**, *167*, 107864. [[CrossRef](#)]
17. Briki, A.; Olmos, E.; Delaunay, S.; Fournier, F. Generalized modelling of effect of oxygenation and glucose concentration on *Corynebacterium glutamicum* growth and production kinetics. *Biochem. Eng. J.* **2022**, *187*, 108577. [[CrossRef](#)]
18. Hefzi, H.; Ang, K.S.; Hanscho, M.; Bordbar, A.; Ruckerbauer, D.; Lakshmanan, M.; Orellana, C.A.; Baycin-Hizal, D.; Huang, Y.; Ley, D. A consensus genome-scale reconstruction of Chinese hamster ovary cell metabolism. *Cell Syst.* **2016**, *3*, 434–443.e438. [[CrossRef](#)] [[PubMed](#)]
19. Helgers, H.; Hengelbrock, A.; Schmidt, A.; Rosengarten, J.; Stitz, J.; Strube, J. Process Design and Optimization towards Digital Twins for HIV-Gag VLP Production in HEK293 Cells, including Purification. *Processes* **2022**, *10*, 419. [[CrossRef](#)]
20. Hengelbrock, A.; Helgers, H.; Schmidt, A.; Vetter, F.L.; Juckers, A.; Rosengarten, J.F.; Stitz, J.; Strube, J. Digital Twin for HIV-Gag VLP Production in HEK293 Cells. *Processes* **2022**, *10*, 866. [[CrossRef](#)]
21. Helgers, H.; Hengelbrock, A.; Rosengarten, J.F.; Stitz, J.; Schmidt, A.; Strube, J. Towards Autonomous Process Control—Digital Twin for HIV-Gag VLP Production in HEK293 Cells Using a Dynamic Metabolic Model. *Processes* **2022**, *10*, 2015. [[CrossRef](#)]
22. Park, S.-Y.; Park, C.-H.; Choi, D.-H.; Hong, J.K.; Lee, D.-Y. Bioprocess digital twins of mammalian cell culture for advanced biomanufacturing. *Curr. Opin. Chem. Eng.* **2021**, *33*, 100702. [[CrossRef](#)]
23. Liu, H.; Li, X.; Qian, J.; Liu, J.; Du, G.; Chen, J. Hydrodynamics and mass transfer in rocking T25 cell culture flasks. *CIESC J.* **2022**, *73*, 1546–1556. [[CrossRef](#)]
24. Wong, B.G.; Mancuso, C.P.; Kiriakov, S.; Bashor, C.J.; Khalil, A.S. Precise, automated control of conditions for high-throughput growth of yeast and bacteria with eVOLVER. *Nat. Biotechnol.* **2018**, *36*, 614–623. [[CrossRef](#)] [[PubMed](#)]
25. Lopez-Meza, J.; Araiz-Hernandez, D.; Carrillo-Cocom, L.M.; Lopez-Pacheco, F.; Rocha-Pizana Mdel, R.; Alvarez, M.M. Using simple models to describe the kinetics of growth, glucose consumption, and monoclonal antibody formation in naive and infliximab producer CHO cells. *Cytotechnology* **2016**, *68*, 1287–1300. [[CrossRef](#)] [[PubMed](#)]
26. Deshpande, R.R.; Heinzle, E. On-line oxygen uptake rate and culture viability measurement of animal cell culture using microplates with integrated oxygen sensors. *Biotechnol. Lett.* **2004**, *26*, 763–767. [[CrossRef](#)] [[PubMed](#)]
27. Hartmann, F.S.; Udugama, I.A.; Seibold, G.M.; Sugiyama, H.; Gernaey, K.V. Digital models in biotechnology: Towards multi-scale integration and implementation. *Biotechnol. Adv.* **2022**, *60*, 108015. [[CrossRef](#)] [[PubMed](#)]
28. Wang, G.; Haringa, C.; Noorman, H.; Chu, J.; Zhuang, Y. Developing a computational framework to advance bioprocess scale-up. *Trends Biotechnol.* **2020**, *38*, 846–856. [[CrossRef](#)] [[PubMed](#)]

**Disclaimer/Publisher’s Note:** The statements, opinions and data contained in all publications are solely those of the individual author(s) and contributor(s) and not of MDPI and/or the editor(s). MDPI and/or the editor(s) disclaim responsibility for any injury to people or property resulting from any ideas, methods, instructions or products referred to in the content.